PELLETIZED LITHIUM–METAL SULPHIDE CELLS
PART II. SOME OPERATING CHARACTERISTICS OF PELLETIZED LiAl–FeS CELLS

M. J. WILLARS and J. G. SMITH

Shell Research Ltd., Thornton Research Centre, P.O. Box 1, Chester CH1 3SH (Gt. Britain)

Summary

A number of small, pelletized LiAl/FeS secondary cells, in which the LiCl–KCl electrolyte is immobilized on the surface of an inert ceramic powder, have been tested over a range of operating conditions. The capacity of such cells is markedly dependent on both cell temperature and discharge current density, an effect attributed to local compositional changes in the binary electrolyte mixture. Measurements of cell resistance and electrolyte re-equilibration phenomena lend support to this argument. The self-discharge rate of cells left on open-circuit was found to be relatively high and sensitive to moisture contamination. The cycle life of these cells, however, is remarkably good, more than 2000 charge/discharge cycles having been completed at a one-hour rate. In such experiments the current efficiency was found to approach 100% and the energy efficiency was about 85%, though the depth of discharge was only 40%.

1. Introduction

The decline in the ability of crude oil to meet the growing demand for energy in the long term will encourage a considerable shift in the pattern of energy production and consumption. Electricity provides a convenient medium for the transport and utilization of energy from alternative sources (such as solar and nuclear power) and is likely to play an increasingly important role in the overall energy scene. Secondary batteries of high specific-energy and high specific-power could become central to the efficient management of an electrically based economy, fulfilling a number of power source and energy storage requirements [1].

The anode and cathode materials capable of meeting these needs are the low atomic weight alkali metals (*e.g.*, sodium and lithium) and the chalcogens (*e.g.*, sulphur and selenium) or halogens (*e.g.*, chlorine and bromine). The inherent reactivity of such materials excludes the use of aqueous electrolytes

in these systems and, in consequence, organic electrolytes have been considered for normal temperature systems [2], and fused salts [3] or solid ionic conductors [4] for systems operating at elevated temperatures. The power density for cells containing organic solvents is low because of the low ionic conductivity of the solutions (typically 10^{-2} ohm^{-1} cm^{-1}). Fused salts, however, provide a highly conducting medium (1 - 4 ohm^{-1} cm^{-1}) allowing specific powers in excess of 200 W kg^{-1} to be achieved [5].

We have recently reviewed the chemistry of lithium/metal sulphide batteries [6]. One of the most promising of such systems presently under investigation is represented by the reaction

$$2LiAl + FeS \underset{charge}{\overset{discharge}{\rightleftharpoons}} Li_2S + Fe + 2Al \qquad (1)$$
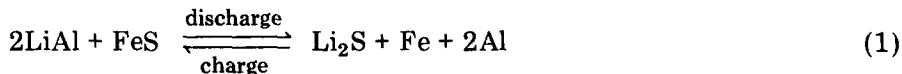
which has a theoretical energy density of 458 W h kg^{-1}, the discharge reaction occurring at ~ 1.30 V.

The lithium chloride/potassium chloride eutectic mixture (m.p. 352 °C) is the commonly used electrolyte and, in consequence, the cells are generally operated at 400 - 500 °C. A great deal of design flexibility and compactness can be gained by immobilizing a thin film of the fused salt electrolyte either in an absorbent matrix or as a rigid paste. The U.K. Admiralty Marine Technology Establishment has described a method enabling cells to be fabricated in the form of pressure-compacted pellets [7, 8], the electrolyte being immobilized by admixture with an inert powder. The resultant disc is robust and can readily be incorporated into a bipolar battery design with no intercell connectors. Pelletizing is not unique, indeed the Argonne National Laboratory in the U.S. has described similar systems [9]. Owing to the presence of inert filler however, the highest current ratings (and, hence, power densities) are reduced compared with the flooded system. Even so, it has been suggested that an energy density of 130 W h kg^{-1} is attainable for a 10 kW h capacity module [10].

This paper describes experiments designed to evaluate the fundamental operating characteristics of small, pelletized LiAl–FeS secondary cells.

2. Experimental

All preparative manipulations and cell performance tests were carried out under a dry argon atmosphere, continuously purified in order to maintain moisture and oxygen concentrations below about 5 ppm.

Cells were constructed from anodes of a 20 wt.% lithium–aluminium alloy and cathodes of ferrous sulphide containing approximately 20% excess iron. The electrolyte layer consisted of an LiCl/KCl eutectic mixture immobilized on particles of magnesia, all individual cell components being dried under vacuum prior to use. Standard test cells were of 8.3 cm^2 cross-sectional area and were fabricated with theoretical capacities of 0.6 A h. The discs were pressed from the component powders generally in a single operation at room temperature forming compacts with less than 30% void volume.

The test discs were held in a fused magnesia retaining ring between molybdenum current collectors. This assembly was then placed inside a stainless steel bolt-up housing, the negative connection being made through the case and the positive *via* a glass–metal sealed lead. The complete unit was then transferred to a tubular furnace and connected up so that operating temperature, charge/discharge rate and cell voltage could be monitored continuously.

Constant current cycling experiments were performed using charge/discharge units which reversed the direction of current flow at pre-set potential limits. Cell potentials were monitored on Y–t recorders, enabling cell capacities to be determined from the time taken to sweep between two potential limits (usually 0.9 V and 1.7 V), and the energy passed to be calculated from a voltage integration trace. Each experiment consisted of (a) 50 cycles at a temperature of 450 °C and a charge/discharge current of 25 mA cm^{-2} (to attain a stable state and check reproducibility), (b) 50 cycles under the new operating regime, and finally (c) a further 50 cycles under the initial conditions (to confirm that no irreversible changes had taken place within the cell).

Self-discharge characteristics were determined by charging cells up to 1.7 V (full charge) before standing on open-circuit for a pre-set time and then measuring the charge required to return to this value. Ohmic polarization data were acquired by employing a current interruption technique, the *IR* drop being recorded on an oscilloscope.

3. Results and discussion

3.1. Galvanostatic cycling

A typical charge/discharge cycle for a 0.6 A h LiAl/FeS cell at 500 °C is shown in Fig. 1. At this discharge rate the cell potential falls from about 1.3 V (immediately following the point of current reversal at full charge) to 0.9 V, which was considered to be the lowest useful output potential, *i.e.*, the "discharged" state. The open-circuit potential of these cells was approximately 1.33 V and in the above experiment driving over-potentials of ∼ 100 mV are recorded at points nearly midway through the charge or discharge.

The current efficiency (*i.e.*, charge recovered on discharge divided by charge introduced during the charging process) as measured from the Y–t recorder was virtually 100% for such cells, and the corresponding energy efficiency was typically 80 - 85%.

The upper and lower voltage limits chosen are designed to satisfy a number of requirements. Secondary reactions are to be avoided (*e.g.*, FeS + Li$_2$S → 2Li + FeS$_2$ which occurs at ∼ 2.0 V) [11] and electrochemical attack on the current collectors and cell housings at high anodic potentials is to be minimized. Also, the resistive and concentration polarization components of the cell voltage increase rapidly near these end points, thereby reducing the overall efficiency of the cycling process.
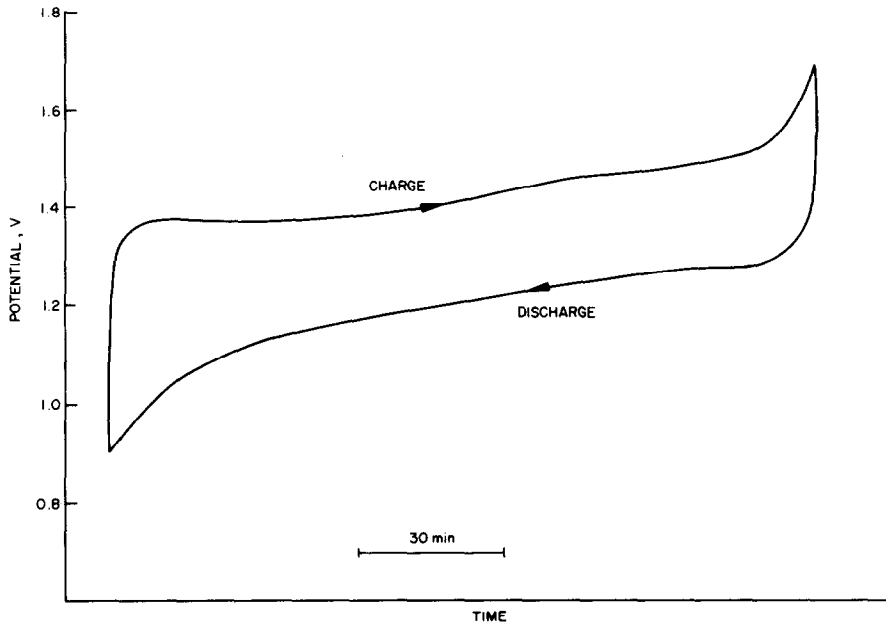
Fig. 1. Typical charge/discharge profile for a 0.6 A h pelletized LiAl/FeS cell operated at 500 °C ($i = 25$ mA cm^{-2}).

Extending the cut-off limits by 100 mV in either direction increases the voltage range by 12.5% and a corresponding increase in capacity is associated with this. Over a 50 cycle test period no decline in performance was noted as a result of such conditions, though whether the long-term stability would be affected by such an operating regime is not yet known.

Under standard operating conditions, however, the cycle-life of these pelletized cells is remarkably good. The results from the latter half of a life test which was terminated after 2000 cycles are given in Fig. 2. The cell capacity remained virtually constant for almost 1600 cycles before the cell was removed and stored in a relatively high moisture content environment for about 60 days. These cell housings were not hermetically sealed and ingress of the atmosphere was possible. On being returned to test, a lower capacity than before was obtained and this behaviour is attributed to the presence of H_2O which may react with both the lithium alloy and the melt. The reduced performance was not a consequence of the thermal cycle, since in previous experiments cells have been repeatedly cooled to room temperature and reheated without incurring any loss in performance.

The very good cycle life observed may well be associated with the structure of the electrodes, which contain a considerable void volume capable of accommodating the shape changes which occur as material is shifted from one electrode to the other and back. It must be pointed out though, that in the above test the percentage of active material utilized was only about 40%, and cycle life data at higher depths of discharge have yet to be measured.
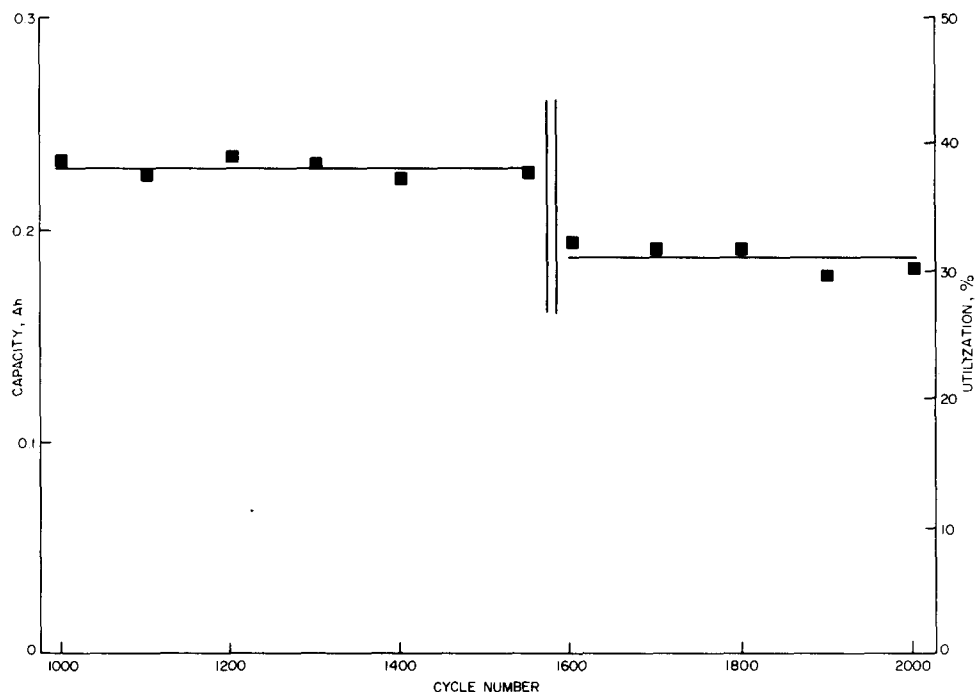
Fig. 2. Cycle life performance of a 0.6 A h LiAl–FeS cell before and after exposure to a high-moisture content environment ($T = 450$ °C, $i = 25$ mA cm^{-2}).

Figure 3 shows a photograph of a cell removed from test after completing more than 450 charge/discharge cycles. Clearly, the integrity of the layered structure is not destroyed by such processes.

3.2. Electrolyte phenomena

The utilization of active materials in the cell (and, hence, capacity) is a function of discharge current density and temperature (Fig. 4). Utilization, in fact, bears an inverse relationship with regard to discharge current density, rising from 16% at 50 mA cm^{-2} to 55% at 12.5 mA cm^{-2}. This behaviour has been interpreted recently [12] in terms of a phase separation effect in the binary electrolyte mixture. At high rates of discharge the concentration gradients generated near reacting surfaces may be of sufficient magnitude to induce crystallization of the KCl component from the melt within the FeS electrode structure. This would lead to the formation of a resistive film, blocking reaction sites. From the electrolyte phase diagram [13] it is possible to predict a temperature dependence of utilization using the model outlined above, and this too is borne out experimentally.

Further support for such a scheme is provided by measurements of cell resistance taken throughout a charge/discharge cycle. Figure 5 shows how ohmic polarization of these cells increases markedly as the end of discharge is approached. The value observed at 0.9 V (end of discharge) is some 30%

Fig. 3. Photomicrograph of a pelletized cell after 450 charge/discharge cycles.

higher than at 1.7 V (end of charge) owing to the formation of solid KCl in the melt (crystals of which have been detected in discharged cells using SEM). After current reversal the resistance falls dramatically and remains at a comparatively low value until the end of charge (when the major contribution to the rising cell potential will be caused by the lack of availability of active material).

Another associated effect is that of electrolyte relaxation which may occur in cells left on open-circuit from the partly or fully discharged condition. When the current flow is interrupted, the polarization-induced compositional changes in the electrolyte will tend to re-equilibrate. Hence, when the discharge is continued an extra quantity of charge will be made available before the freezing condition is realized in the melt. The capacity enhancement is retained for a further 40 cycles following such an experiment (Fig. 6) before the equilibrium value is regained.

3.3. Self-discharge

An accurate measure of coulombic efficiency for the cell cycling process was obtained by employing a digital coulometer to determine the *net* charge passed during 70 h of a continuous cyclic test. A charge loss equivalent to a constant self-discharge current of 0.4 mA was recorded, and this translates to an overall current efficiency of 99.8% under those experimental conditions (*i.e.*, 450 °C, $i = 25$ mA cm^{-2}).

The behaviour of cells left on open-circuit at 450 °C was studied by charging cells up to 1.7 V, breaking the source/sink circuit for a set length of time and then measuring the amount of charge necessary to regain the fully charged state. The results for two such tests are given in Fig. 7. Curve (a) cor-
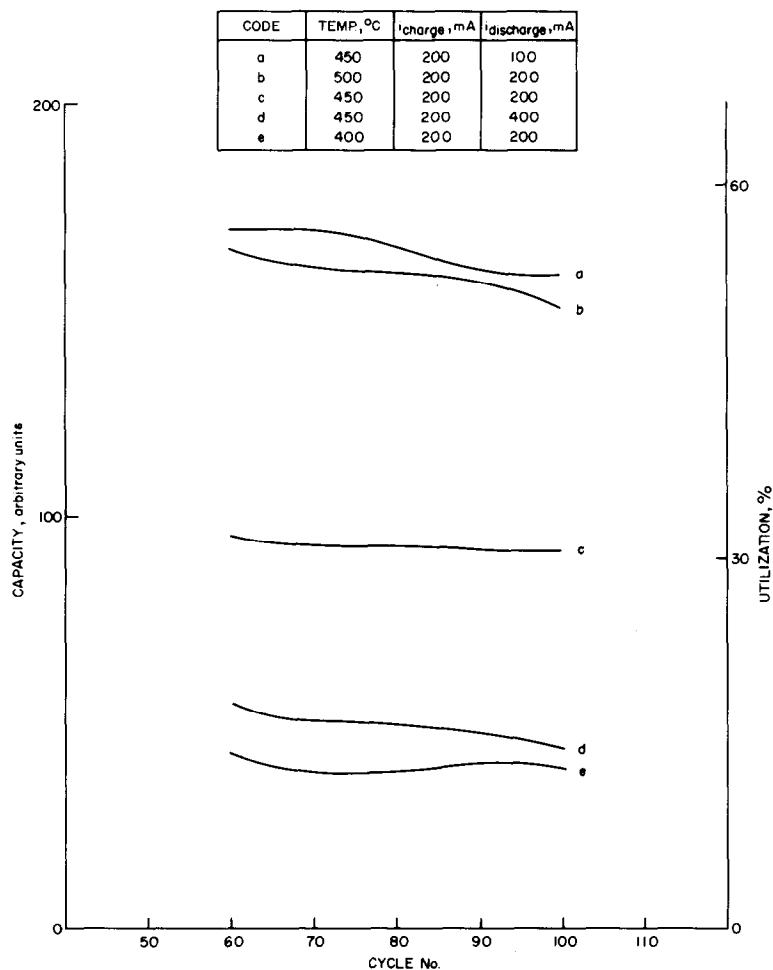
CODE	TEMP,°C	I_{charge}, mA	$I_{discharge}$, mA
a	450	200	100
b	500	200	200
c	450	200	200
d	450	200	400
e	400	200	200

Fig. 4. The effect of operating temperature and discharge current on the capacity of pelletized LiAl–FeS cells.

responds to a cell that had completed $\sim$ 2000 cycles over a 30 week period (and had been exposed to a relatively high moisture-content environment leading to a reduced output capacity), and curve (b) to a relatively new cell after only 200 cycles and 3 weeks on test. The data from curve (b) are in line with the aforementioned value of 0.4 mA for self-discharge current and a comparison of the two curves illustrates the sensitivity of the system to contamination. The rate of capacity loss is nearly three times as high in the aged cell.

This magnitude of current cannot be attributed solely to the known electronic conductivity of the LiCl/KCl electrolyte [14] for which a leakage rate of less than 0.2 mA would be expected. The presence of Li_2O_2 resulting from an ingress of moisture, however, markedly increases the conductivity of the melt [15], and could account for the differing performances observed.
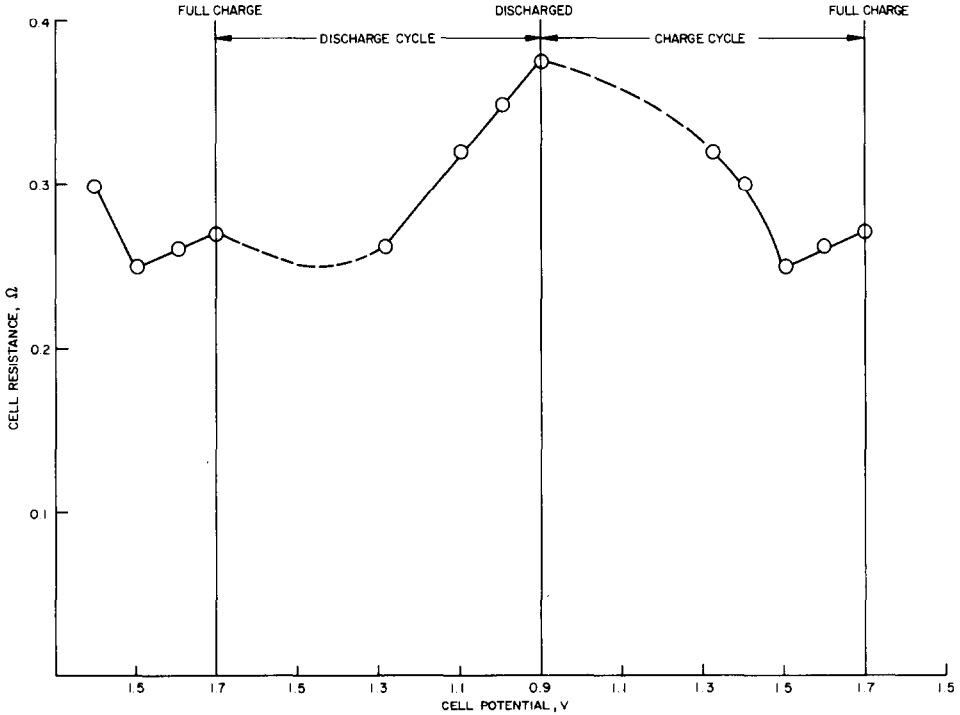
Fig. 5. Variation of cell resistance throughout a test cycle for an LiAl–FeS cell at 450 °C. (A = 8.3 cm^2.)
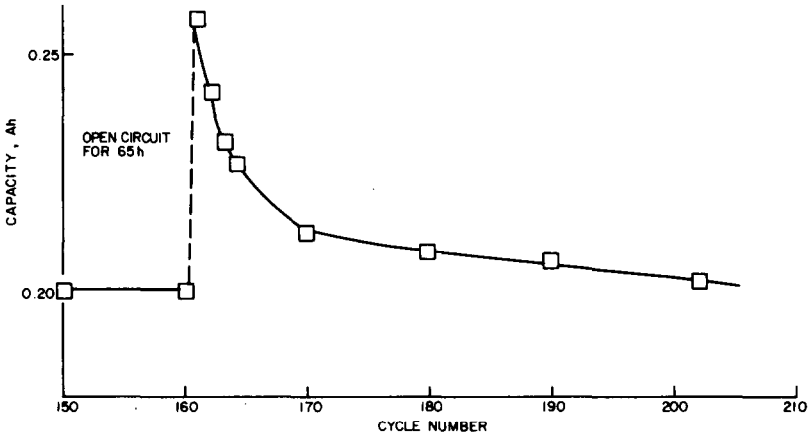

Fig. 6. Capacity enhancement effect exhibited by pelletized cells following a period of 65 h on open-circuit in the fully discharged condition.

When cooled to room temperature, the mixed salt electrolyte solidifies and its conductivity is significantly reduced. Consequently, self-discharge currents become negligible. In fact all of the capacity loss during tests of this nature can be accounted for by assuming that the processes responsible for
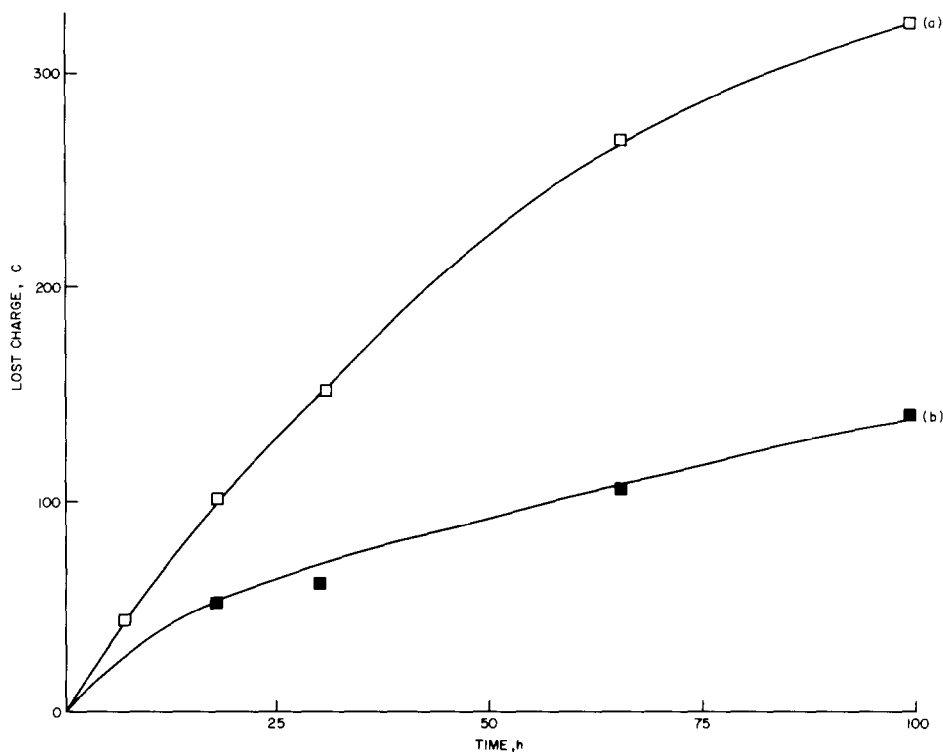
Fig. 7. Rate of charge loss for cells left on open-circuit at full charge (T = 450 °C). (a) After 2000 cycles (~ 30 weeks on test); (b) after 200 cycles (~ 3 weeks on test).

the self-discharge occur only when the electrolyte is molten (*i.e.*, during the finite cooling and re-heating periods). Thus, pelletized cells may be stored at ambient temperature indefinitely without incurring a serious loss of charge.

These data yield important implications regarding the applicability of this system to various modes of operation. The low rate of charge loss for cells stored at room temperature for long periods represents a useful feature, as does the proven ability to withstand repeated thermal cycling. However, the high rate of charge loss at operating temperature suggests that these cells would operate most effectively under a regime of continuous charging and discharging. Standby applications and those in which charging periods may be sporadic (*e.g.*, in photovoltaic support systems) would require much lower rates of self-discharge.

4. Summary and conclusions

Lithium aluminium/iron sulphide secondary cells containing an immobilized LiCl–KCl electrolyte have been tested over a wide range of operating conditions. The open-circuit potential of such pelletized cells is approximately 1330 mV at 450 °C, but under load this steadily falls from 1.3 V near full charge to 0.9 V when the cell is considered to be discharged.

At one-hour charge and discharge rates (25 mA cm^{-2}), these cells are capable of undergoing more than 2000 cycles of operation. The coulombic and energy efficiencies of the cycling process are approximately 100% and 85%, respectively, and the active materials utilization is 40% (though this may fall if moisture is not rigorously excluded from the cell).

The dependence of capacity on current density and operating temperature can be rationalized by assuming that a phase separation of KCl from the electrolyte limits the discharge. In support of this argument, cell resistances are seen to increase near the end of discharge and relaxation effects associated with the melt are observed.

When left on open-circuit at 450 °C the capacity loss in this type of cell is relatively high (approximately 0.5% per hour in the early stages but with the rate falling rapidly), but as a result of the loss in melt conductivity virtually no charge is lost from cells cooled to room temperature. These observations suggest that in their present form, such pelletized cells would be most suited to applications in which the charging and discharging operations are predictable and regular (*e.g.*, load levelling).

Acknowledgement

References

1 J. D. Busi and L. R. Turner, *J. Electrochem. Soc., 121* (1974) 183C.
2 See, for example, G. Eichinger and J. O. Besenhard, *J. Electroanal. Chem., 68* (1976) 1.
3 See, for example, D. M. Bush and D. A. Nissen, *Proc. 28th Power Sources Conf., Atlantic City, N.J., 1978,* p. 81.
4 See, for example, G. R. Lomax, *J. Power Sources, 4* (1979) 301.
5 H. Shimotake and E. J. Cairns, *Adv. in Energ. Conv. Eng.,* Am. Soc. Mech. Eng., New York, 1967, p. 951.
6 R. W. Glazebrook and M. J. Willars, *J. Power Sources, 8* (1982) 327.
7 Improvements in or relating to high temperature secondary batteries, *U.K. Patent 1,510,642* (1978).
8 High temperature secondary cell, *U.K. Patent 1,583,981* (1981).
9 H. Shimotake, G. L. Rogers and E. J. Cairns, *Ind. Eng. Chem., Proc. Des. Dev., 8* (1969) 51.
10 D. R. Feltham, G. Hazzard and L. Pearce, in J. Thompson (ed.), *Power Sources 7,* Academic Press, London and New York, 1979, p. 691.
11 D. R. Vissers, Z. Tomczuk and R. K. Steunenberg, *J. Electrochem. Soc., 121* (1974) 665.
12 See, for example, M. J. Willars, J. G. Smith and R. W. Glazebrook, *J. Appl. Electrochem., 11* (1981) 335; R. Pollard and J. Newman, *J. Electrochem. Soc., 128* (1981) 491.
13 E. Elchardus and P. Lafite, *Bull. Soc. Chim. Fr., 51* (1932) 1572.
14 R. J. Heus and J. J. Egan, *J. Phys. Chem., 77* (1973) 1989.
15 R. Knödler, G. Gohme and W. Borger, *J. Electrochem. Soc., 127* (1980) 1311.